ISIJ International, Vol. 30 (1990), No. 1, pp. 48-57

Heat Transfer Analysis during Water Spray Cooling of Steel Rods

R.D. MORALES, A.G. LÓPEZ and I.M. OLIVARES[1)]

Department of Metallurgy, ESIQIE-Instituto Politécnico Nacional, C.P. 07360 México D.F., México. 1) Puebla Steelworks, HyLSA, Sn. Miguel Xoxtla, Puebla, México.

(*Received on April 17, 1989; accepted in the final form on September 8, 1989*)

A mathematical model has been developed to predict the rod cooling behavior of steel rods under the action of water sprays in the precooling system of a Stelmor machine. The main objective of this work was to study the influence of operation parameters such as rod size, rod speed, rod temperature at the finishing mill, water flow-rate and spray cooling sequence on the final temperature distribution within the rod before it enters into the transformation conveyor.

This heat transfer analysis indicates that the spray cooling sequence affects, considerably, the temperature distribution inside the rod. Besides, water flow-rate failures in the spray cooling system disturb drastically its cooling efficiency. Finally, reheating phenomena which go from 150 to 200°C at rod surface are predicted. The calculations were validated with *in situ* experimental measurements carried out at HyLSA's (Puebla Plant) Stelmor machine. Very good agreement was found between predicted and experimentally measured rod surface temperatures.

KEY WORDS: steel; rod; water-spray; cooling-rate reheating; Stelmor Process; flow-rate; heat-transfer; finishing mill; wire; drawing; speed; pearlitic transformation.

1. Introduction

The cooling rate of steel rods in a precooling system of a Stelmor machine (employed for steel rod patenting) depends on various operation parameters. Among those parameters the most important are rod size, rod speed (finishing speed), rod temperature at the finishing mill, water flow-rate and spray cooling sequence.

For some given operation conditions, the cooling rate will set a temperature distribution within a steel rod just before it enters into the transformation conveyor (Laying temperature). Since the transformation from austenite to pearlite (or pearlite plus ferrite) should take place in a 33 m long forced air cooled zone (Fig. 1) this temperature becomes very important for the process performance. If this temperature distribution is high (low efficiency of the precooling system) there is a danger that the solid state transformation within the rod may finish outside the forced air cooling zone. This will enable the precipitation of a coarse pearlite which will decrease the mechanical properties of the product.[1)]

Moreover, very high cooling rates at the precooling system may induce the precipitation of metastable phases like bainite or martensite. Under these possible circumstances the rod will become useless for patenting and final drawing operations.

On the other hand, a right rod cooling rate by water, immediately after completion of rolling, preserves to a large extent the refinement of the austenitic grain structure produced by hot deformation, making the steel more responsive to the subsequent patenting operations.

Consequently, in order to control the rod cooling rate at this precooling system, hereinafter called Rapid Cooling System (RCS), a mathematical model which involves all operation parameters above mentioned will be developed in the following lines.

2. The Mathematical Model of the RCS

The technical specifications of this precooling system for HyLSA's Stelmor machine indicate that it is capable of cooling steel rods from finishing temperatures as high as 1 040 to 785°C during the time required to travel 30 m at mill delivery speeds from 12 to 42 m/s for different rod diameters.

As can be seen in Fig. 1, it is possible to divide the heat transfer mechanisms into 5 zones at the RCS. In this RCS the steel rod is cooled down to a desired laying temperature without the presence of a phase transformation. This precooling system brings the rod nearer to the pearlitic transformation starting temperature.

These zones have the following characteristics:

Zone 1: This zone (3 m long) comprises from the last finishing roll of the mill to the first water cooling box. The heat transfer mechanism is that of radiation from the rod surface to the surroundings.

Zone 2: This zone (8 m long) belongs to the first cooling box (the first spray cooling stage), which has in its inside 4 water sprays uniformly distributed along its length. The heat transfer mechanism is a combination of forced convection, owing to the presence water sprays, and by radiation through the water vapor film formed at the rod surface. Both mechanisms are considered to work simultaneously during the rod passage through this zone.

Zone 3: This a 8 m long zone whose main function

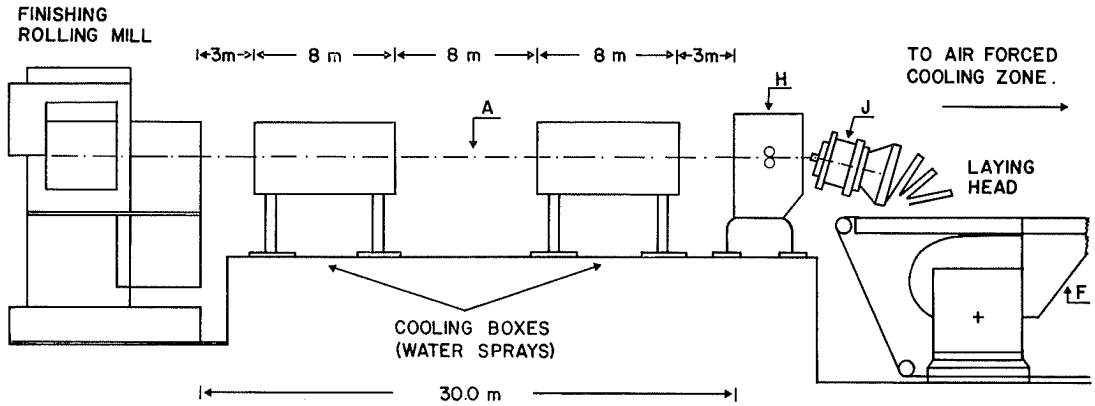

Fig. 1. Rapid Cooling System of HyLSA's Stelmor machine.

is to equilibrate the rod center and surface temperatures (a temperature gradient is promoted by the preceding spray cooling zone) through a free radiation to the surroundings. However, owing to the high rod delivering speeds at the last roll of the finishing mill, a visible vapor film of water is dragged along the rod traveling direction. Table 1 shows the usual rod delivering speeds for different rod sizes. Consequently, the heat transfer mechanism is considered to be, also, a combination of radiation and convection.

The first layer of fluid in contact with the rod surface is a water vapor film, next to this, there are other layers of liquid water with different saturation degrees.

During the residence time of the rod in this zone it is assumed that the heat transfer mechanism is similar to that when a hot steel rod is submerged into a pound of liquid water as in quenching processes. Consequently, the heat is extracted by convection owing to the movement of the vapor–liquid mixture and by radiation through the vapor film as it is well explained in some textbooks.[2)]

Zone 4: This zone (8 m long) comprises the second cooling box (the second spray cooling stage). This box has, also, 4 water sprays uniformly distributed along its length. The heat extraction mechanism is similar to that already explained for the first cooling box, (zone 2).

Zone 5: This zone belongs to the length from the end of the second cooling box to the wheel guide of the laying head (see Fig. 1) where the heat transfer mechanism is again the same as that of zone 3. This zone is the second temperature equilibration zone (TEZ 2).

Besides, owing to the high speeds of motion of the rod, conduction along the rod is negligible in comparison with heat flow by bulk motion.

Additionally, as the rod diameter is much smaller than its length, it is possible to assume heat flow mainly through the radial direction of the unsteady heat conduction equation:

$$\frac{\partial}{\partial r}\left(k\frac{\partial T}{\partial r}\right)+\frac{k}{r}\left(\frac{\partial T}{\partial r}\right)=C_p\rho\frac{\partial T}{\partial t} \quad \text{.....(1)}$$

C_p and k are dependent on the temperature, but as it is observed in Fig. 2 these thermophysical properties for an eutectoid steel (or any other carbon steel) can be straight line adjusted by equations of the type.[3)]

Table 1. Rod speeds at the finishing mill and at the conveyor.

Rod radius (m)	Finishing speed (m/s)	Conveyor speed (m/s)	Temperature at the laying head (°C)
0.0031	40.1	0.80	950
0.0031	42.0	0.70	950
0.0040	31.0	0.63	925
0.0044	27.0	0.63	925
0.0048	24.0	0.60	900
0.0051	19.0	0.60	900
0.0055	14.0	0.60	870
0.0060	12.0	0.60	870

$$k=A+BT \quad \text{.....(2-a)}$$

$$C_p=A'+B'T \quad \text{.....(2-b)}$$

where, A, B, A', B': constants.

Eq. (1) is solved together with initial and boundary conditions according to the following easily derived equations,

i) at $r=r$ and $t=0$ $\quad T=T_i$ .....(3)

ii) at $r=0$ and $t=t$ $\quad \dfrac{dT}{dr}=0$ .....(4)

iii) at $r=R$ and $t=t$ $\quad -k\dfrac{\partial T}{\partial r}=\sigma\varepsilon(T^4-T_a^4)$ .....(5)

iv) at $r=r$ and $t=t^*$ $\quad T=f(r,t^*)$ .....(6)

v) at $r=R$ and $t=t$ $\quad -k\dfrac{\partial T}{\partial r}=h(T-T_w)$ .....(7)

The solution of Eq. (1) gives the temperature profile in a transverse slice of steel rod that travels through the RCS from the last roll of the finishing mill (finishing block) to the wheel guide at the laying head. Space and time are related through $s=Vt$ where V is the rod traveling speed at the RCS.

The initial condition, Eq. (3), assumes that the temperature in the cross section of the rod leaving the last roll of the finishing mill is uniform. Eq. (4)

establishes the temperature profile symmetry.

Eqs. (1), (3) to (5) are numerically solved for the zone 1.

Eq. (6) is some kind of initial condition at a time (t^*) corresponding to the starting of every cooling zone after the first one. At the starting time of a given zone (t^*) (including from the second to the fifth zone), the temperature vector $f(r, t^*)$ resulting from a preceding zone is substituted in Eq. (6). In this way the system of equations is solved employing Eq. (6) with $T=f(r, t^*)$ instead of Eq. (3) and Eq. (7) instead of the boundary condition (5). The heat-transfer coefficient in Eq. (7) will change according to the heat transfer mechanism operating in a given zone as will be explained latter.

For calculating the temperature profiles in the zones 2 and 4, Eqs. (1), (4), (6) and (7) are solved making use of a dummy vector (N,N,N,N) for the two cooling boxes, where N has only two values, 1 or 0. In the first case, it indicates that the corresponding spray is working and in the latter that the corresponding spray is off. As an example the spray sequence (0,1,1,0); (0,0,0,1) indicates that the second and the third sprays of the first box and the fourth spray of the second box are working, whereas the rest are closed.

The heat-transfer coefficient h in Eq. (7) is in formal terms some kind of a pseudo heat-transfer coefficient since it involves combined heat transfer mechanisms of forced convection and radiation working simultaneously in zones (2) to (5).

In order to estimate the value of h, it is necessary to take into consideration that zones 2 and 4 are fundamentally cooled by water sprays, while zones 3 and 5 by radiation and by the dragged water film along the traveling direction of the rod. Consequently, the heat-transfer coefficient by forced convection hc, involved in h, should be calculated through two different methods for zones 2 to 4 and zones 3 to 5, respectively.

2.1. *Calculation of the Heat-transfer Coefficient for Zones 2 and 4*

Most of the experimental work on the determination of heat-transfer coefficient has been done in the laboratory, using hot steel plates, typically 3 m square, using commercial nozzles. There are not systematic reports on heat-transfer coefficients of hot steel rods-water spray systems. Thus, in order to find out a heat-transfer coefficient whose value may give the best fit with the experimental observations, it is the only available way, to limit the search to hot steel plates-water spray systems usually given by empirical correlations.

Spray heat-transfer coefficients are strongly affected by variables such as nozzle type, nozzle size, water flux, water pressure and nozzle-steel distance, surface tempeature, *etc.* These variables can be divided into two categories depending on whether or not they influence the spray water flux (l/m^2 s) which is the most important spray variable. Then the effect of variables such a nozzle type, water pressure and nozzle-steel surface distance on spray heat-transfer coefficient can be seen primarily in terms of their effect on the spray water flux whereas variables like water temperature and steel surface temperature affect the heat-transfer coefficient directly.

Under these grounds it is better to look for correlations involving the most immediate variables such as water flux, water temperature and pressure. These correlations should be applicable for steel surface temperature of 800–1 100°C and for water temperatures such as 20–30°C. These conditions point out that the cooling phenomenon is under the regime of unstable film boiling.[4]

Mitsutsuka[5] evaluated the experimental data of various workers under film boiling regime assuming that the heat-transfer coefficient is a function of the most direct variables, water flux, water temperature and steel surface temperature.

In Table 2 the experimental conditions employed by those researchers[6,15] for the estimation of the heat-transfer coefficient are summarized. From a statistical analysis of all reported data Mitsutsuka found the first correlation reported in Table 3. In this same Table there are some other correlations determined by various authors such as Sasaki,[12] Ishiguro,[16] Nozaki *et al.*,[17] Bolle and Moreau,[18,20] Shimada and Mitsutsuka,[19] and Mizikar[9] given by Eqs. (B), (C), (D), (E), (G), (F), (H) and (I), respectively.

In addition of these equations, the Iron and Steel Institute of Japan[21] gives Eqs. (J) and (K) based on the results of various experimental works. It is important to point out that these eleven equations are the results of at least 20 of the most relevant works reported in the field and consequently they should be considered as a good source of heat-transfer-coefficient data for spray-hot steel surface systems under film boiling regime.

All equations in Table 3 were tried in the model and compared with experimental temperature measurements, to determine the suitable one for the plant.

A pseudo heat-transfer coefficient for radiation heat-transfer was estimated by,[21]

$$h_r = 4.5333\left[\left(\frac{T_s+273}{100}\right)^4-\left(\frac{T_w+273}{100}\right)^4\right]\Big/(T_s-T_w) \quad \text{.....(8)}$$

In this equation the emissivity of the steel has been assumed to be equal to 0.8. The combined heat-transfer coefficient is given simply by,

$$h = h_c+h_r \quad \text{.....(9)}$$

2.2. *Calculation of the Heat-transfer Coefficient for Zones 3 and 5*

As the rod surface temperature at the RCS is still very high the heat transfer mechanism in these zones belongs also to that of unstable film boiling regime. According to this mechanism the heat-transfer coefficient for convection heat flow is given by[22]

$$h_c = 0.62\left[\frac{H_v'\rho g(\rho_1-\rho)k^3}{\mu(T_s-\bar{T}_{sat})D}\right]^{1/4} \quad \text{.....(10)}$$

Table 2. Test conditions for the estimation of heat-transfer coefficients.[5]

Heat transfer state	Researchers	Specimen conditions			Water flux ($l/m^2 \cdot min$)
		Material	Size (mm)	Heating temperature (°C)	
Steady	Junk[6]	Heat resisting steel	$2.5 \times 83 \times$ (100 to 250)	800 to 1 300	Unknown
	Muller and Jeschar[7]	Heat resisting steel	(6 to 10)×(20 to 60)×L	800 to 1 200	18.6 to 546
Unsteady	Mitsusuka[8]	Carbon steel	$28 \times 220 \times 220$	Max. 930	5 to 2 000
	Mizikar[9]	Stainless 18Cr-8Ni steel	$16 \times 127 \times 127$	Max. 1 094	163 to 1 400
	Mitsusuka and Fukuda[10]	Carbon steel	(22 to 51)×550×1 000	Max. 630	5 to 100
	Hoogendoorn and den Hond[11]	Stainless 18Cr-8Ni steel	$25 \times 185\phi$	Max. 1 000	36 to 1 500
	Sasaki *et al.*[12]	Stainless 18Cr-8Ni steel	$30 \times 300 \times 300$	Max. 1 200	100 to 2 500
	Kamio *et al.*[13]	Steel	$40 \times 60 \times 130$	Max. 1 100	51 to 1 130
	Amano and Kunioka[14]	Steel	$20 \times ? \times ?$	Max. 900	600
	Ohtomo *et al.*[16]	Steel	3 to $10 \times ? \times ?$	Max. 800	1 000 to 30 000

Table 3. Heat-transfer coefficient for spray cooling systems. (kW/m^2K)

Eq.	Correlation	Ref. No.	Observations
(A)	$h_c = 2.6612 \times 10^5 W^{0.616} / T_s^{2.445}$	5)	W in $l/m^2 \cdot min$, T_s, steel temperature in °C
(B)	$h_c = 708 W^{0.75} T_s^{-1.2} + 0.116$	12)	W in $l/m^2 \cdot s$, T_s, steel temperature in °C
(C)	$h_c = 0.581 W^{0.451}(1 - 0.0075 T_w)$	16)	W in $l/m^2 \cdot s$, T_w, °C (water temperature)
(D)	$h_c = 1.57 W^{0.55}(1 - 0.0075 T_w)\left(\frac{1}{\alpha}\right)$	17)	W in $l/m^2 \cdot s$, T_w, °C (water temperature), $\alpha = 4$
(E)	$h_c = 0.423 W^{0.556}$	18)	W in $l/m^2 \cdot s$
(F)	$h_c = 1.57 W^{0.55}(1 - 0.0075 T_w)$	19)	W in $l/m^2 \cdot s$, T_w, °C (water temperature)
(G)	$h_c = 0.360 W^{0.556}$	20)	W in $l/m^2 \cdot s$
(H)	$h_c = 0.0776 W$	9)	W in $l/m^2 \cdot s$
(I)	$h_c = 0.1 W$	9)	W in $l/m^2 \cdot s$
(J)	$h_c = 1.1611 \times 10^{-3}$ antilog $(0.663 \log W - 0.00147 T_s)$	21)	W in $l/m^2 \cdot min$, T_s, steel temperature in °C
(K)	$h_c = 1.611 \times 10^{-3}$ antilog $(2.030 + 0.793 \log W - 0.00154 T_s)$	21)	W in $l/m^2 \cdot min$, T_s, steel temperature in °C

where, H': an effective heat of vaporization of water
k, D: the thermal conductivity and diameter of the rod, respectively
μ, ρ_1: its viscosity and density, respectively
ρ: the vapor density.

H_v' is related to the heat of vaporization of water (H_v) through

$$H_v' = H_v\left[1 + \frac{0.4 C_p (T_s - T_{sat})}{H_v}\right]^2 \quad \text{.....(11)}$$

The expressions (8) and (10) are substituted in Eq. (9) to obtain the combined heat-transfer coefficient for zones 3 and 5. The thermophysical properties of water[23] together with those of an eutectoid steel presented in Fig. 2, were adjusted to give simple equations valid in the temperature range where the RCS works. These correlations are reported in Table 4.

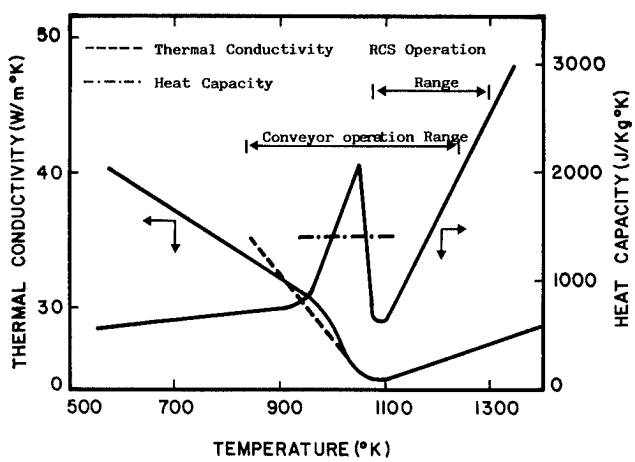

Fig. 2. The thermophysical properties as functions of temperature for eutectoid steels.

3. Numerical Solution

A finite difference method was employed to solve the partial differential equation (1) with its initial and boundary conditions. A slice of the rod was divided into nodes and the temperature profile at each successive time step, which also corresponds to a new position along the RCS line, was calculated using the implicit difference method. The time–position dependent thermophysical properties of steel and water in a given node for a fixed time step, were calculated through the correlations reported in Table 4 at the calculated temperature of the preceding node. The error involved in this approximation is diminished by increasing the number of nodes in the mesh and by making the time steps small enough.

The computing program was coded in Basic and run on a HP-9816 computer of the process metallurgy group at ESIQIE-IPN, Department of Metallurgy.

The structure of the computing program gives a high flexibility to simulate any operational condition including changes in the precooling operation parameters, malfunctions and partial or total equipment

Table 4. Thermophysical properties employed in the model.

Property	Unit	Phase	Correlation	Observation
Viscosity	Pa•s	Water vapor	$\mu=3.5068\times10^{-8}T-6.022\times10^{-7}$	T in °K, valid for $380\leq T\leq1\,000$
Heat capacity	$\frac{J}{Kg°K}$	Water vapor	$C_p=4\,067-102.92\times10^{3}/T^{1/2}+966.50\times10/^{3}T$	T in °K
		Steel	$C_p=493.71+2.3T$	$1\,075°K\leq T\leq1\,350°K$
			$C_p=1\,400$	$950\leq T\leq1\,075°K$
			$C_p=281.4+0.5066T$	$550\leq T\leq950°K$
Thermal conductivity	$\frac{J}{m°K\cdot s}$	Water vapor	$K=C_p\mu$	μ in Pa•s
		Steel	$K=75.42-0.047T$	$830\leq T\leq1\,075°K$
			$K=9.84+0.013T$	$1\,075\leq T\leq1\,350°K$
Density	kg/m³	Water vapor	$\rho=244.75387(T)^{-1.01645}$	T in °K
		Steel	$\rho=7\,850$	Constant
Heat of vaporization	J/kg	Water vapor	$H=-2\,576.57T+32.11\times10^{5}$	T in °K

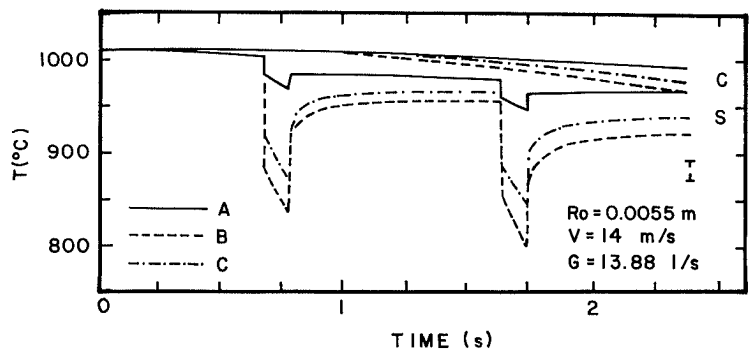

Fig. 3.
Test of the RCS model with Eqs. (A) to (C) for the estimation of the heat-transfer coefficient using a spray sequence (0, 0, 0, 1); (1, 0, 0, 0).

failures. It can be used for the design of rod steel precooling practices and the correction of possible wrong cooling conditions improving the rod laying temperature control at the wheel guide.

4. Comparison of In-plant Measurements with Model Predictions

Two color Modline infrared pyrometers with a wavelength equal to 0.90 μ were located at the exit of the last roll of the finishing mill and at the entrance of the wheel guide, at the laying head respectively. During the operation, the emissivity of these pyrometers was set at 0.8. The pyrometers were, previously, calibrated against an internal black body calibration system.

During the processing of a steel heat, under some determined operation conditions, from 5 to 10 readings were taken from these pyrometers and the average of these readings was reported as a final temperature record.

5. Simulation Results

According to the design of the RCS of this Stelmor line, the flow-rate of water per spray is 13.88 l/s and this value is employed to calculate the water flux, taking into account the number of working sprays in a given cooling box.

Moreover the correlations in Table 3 were employed in the RCS model for calculating h_c in order to find which of them is able to predict the in plant rod surface temperatures with an acceptable accuracy.

Fig. 3 shows the model predictions employing the correlations (A) to (C) under the operating conditions indicated in the same figure. Eqs. (A) to (C) predict considerably higher temperatures at the laying head than the experimental observations. It is interesting to point out that in spite that Eq. (A) is a final result correlated from many experimental works it is not very helpful to estimate the temperature profile for this spray-hot rod steel surface system. The shape of the calculated temperature profiles is typical of spray-hot steel surface systems (*i.e.*, secondary cooling in continuous casting). After the rod enters in a spray working zone there is a sudden temperature decrease at its surface. Once the rod leaves a working spray to enter to a non-working spray zone there is a pronounced surface reheating process assisted by heat flow from the rod center to its surface. On the other hand, the rod center is slightly affected and its temperature decreases only few degrees under the specified operating conditions. Since the residence time of the rod at the RCS is usually very short (in this case 2.35 s) the control of the spray cooling system is a very important operation parameter for subsequent patenting operations.

The test of the model employing Eqs. (D) to (F) is shown in Fig. 4. The first two equations predict higher temperatures than the experimental results while Eq. (E) predicts lower ones. This latter equation makes the model to predict very pronounced cooling-reheating processes at the rod surface. Would this correlation hold for the experimental measure-

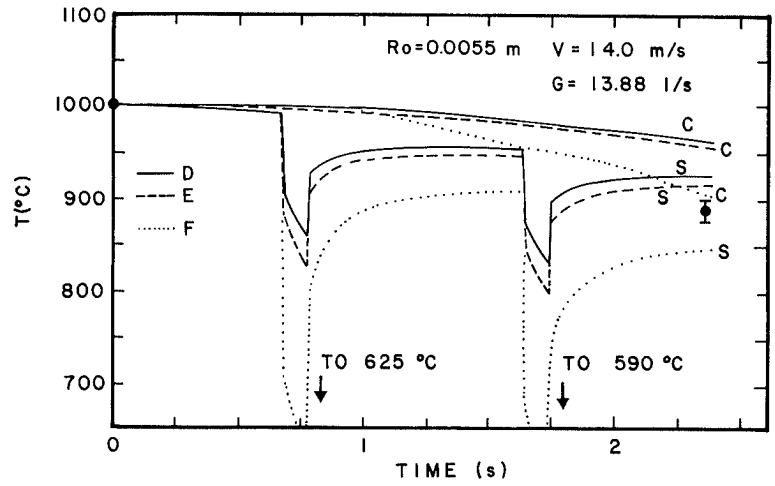

Fig. 4.
Test of the RCS model with Eqs. (D) to (F) for the estimation of the heat-transfer coefficient using a spray sequence (0, 0, 0, 1); (1, 0, 0, 0).

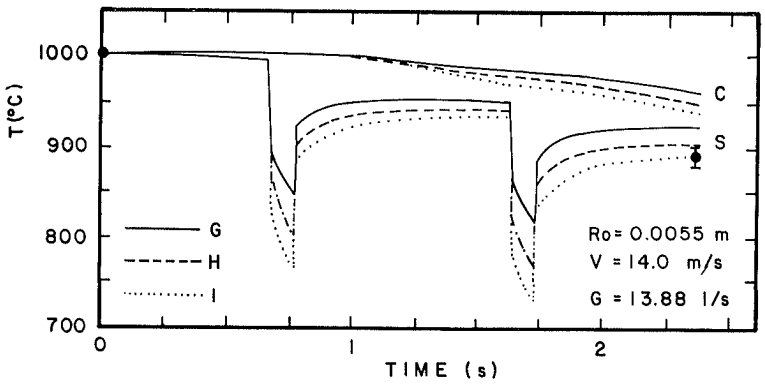

Fig. 5.
Test of the RCS model with Eqs. (G) to (I) for the estimation of the heat-transfer coefficient using a spray sequence (0, 0, 0, 1); (1, 0, 0, 0).

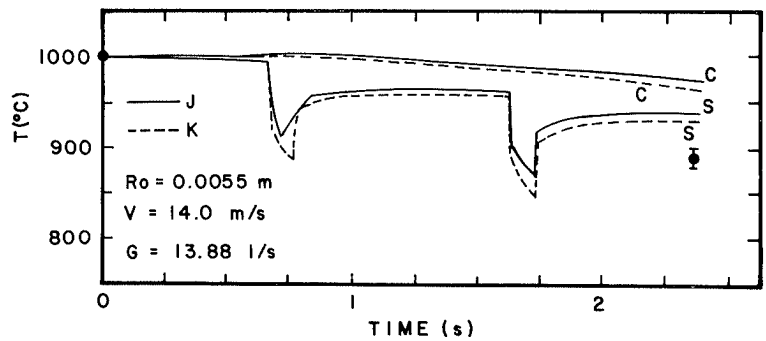

Fig. 6.
Test of the RCS model with Eqs. (J) and (K) for the estimation of heat-transfer coefficient using a spray sequence (0, 0, 0, 1); (1, 0, 0, 0).

ments, the quenching of the rod will be unavoidable even for one working spray.

Fig. 5 shows the computing results employing Eqs. (G) to (I) from Table 3. The first equation makes the model to predict higher temperatures than the experimental measurements. The employment of the second equation predicts closer values but still slightly higher, while the last equation predicts, with excellent accuracy, the observed rod temperature at the laying head.

Thus, the temperature profile calculated by using the correlation (I) in the boundary condition for h_c can be considered as a reliable one to study the thermal flow during the cooling of the rod at the RCS. According to this profile, the first spray decreases the rod surface temperature from 1 000°C at the exit of the last roll of the finishing mill to 760°C at the end of the first working spray. As a consequence the rod surface suffers a reheating from 760 to 940°C (ΔT= 180°C). The second working spray cools the rod surface down to 725°C and the reheating goes up to 900°C (ΔT=175°C) at the end of the RCS, at the laying head. The rod center decreases its temperature from 1 000 to 950°C at the end of the RCS (ΔT= 50°C), at the laying head, owing to the action of the two working sprays for this specific case. The temperature gradient is very high in the neighborhoods of the rod surface indicating that essentially the rod surface and its immediate neighborhood are the only places where extreme cooling-reheating cycles can be expected.

The computing results based on Eqs. (J) and (K) for calculating h_c in the corresponding boundary condition, Eq. (7), are presented in Fig. 6, both correlations make the model to predict considerably higher temperatures than those corresponding to the experimental measurements.

From all those results it can be concluded that the

employment of the correlation (I) (Table 3) in the model gives the best agreement between computed results and the experimental temperature measurements. In the reported computing results hereinafter Eq. (I) will be used to calculate h_c which together with h_r (Eq. (8)) gives the heat transfer coefficient h, in Eq. (7).

To test the validity of Eq. (I), the model was run the simulate different cooling conditions using spray sequences such as (0,0,0,1); (1,1,0,0) and (0,0,0,1); (0,0,0,0), for a rod radius of 0.006 m and a rod traveling speed equal to 12 m/s. From Fig. 7 it is evident that the model predictions coincide excellently with the experimental measurements in both cases. From the comparison of Figs. 5 and 7 for 2 and 3 working spray cooling conditions respectively it is clear that the rod center temperature is only 10°C higher in the first case although their respective surface temperatures are quite different. Evidently, the lower the surface temperature is, the lower will be the rod center temperature equalized at the laying head.

As an example of an extreme cooling operation at the RCS, Fig. 8, where the spray cooling sequence is (1,1,1,1); (1,1,0,0), is very illustrative. The first 4 sprays decrease the rod surface temperature from 1 010°C down to 665°C. Nevertheless, a very strong reheating is generated producing an increase at the surface temperature up to 885°C (ΔT=200°C). The next 2 sprays make the rod surface temperature to decrease down to 649°C and then reheating itself up to 810°C (ΔT=161°C). At the end of this cooling–reheating cycle the rod center temperature reaches 870°C just at the laying head. As was mentioned above, both temperatures (center and surface) will become closer each other at the laying head position.

Once more, these extreme operating conditions are excellently simulated as it is evident from the close agreement between the measurements and the computed temperature at the end of the RCS. In the same Fig. 8 the computed temperature profiles at 1 and 2 mm from the rod surface are drawn and looking at these results it is possible to get a quantitative idea about the promoted high temperature gradient. In fact, these extreme cooling conditions might lead to a quenching process obtaining non-equilibrium phases such as bainite or martensite which will make the rod useless for wire drawing operations. For example, extreme cooling conditions should be avoided for small diameter rods even if their residence times at the RCS are smaller than that shown in Fig. 8.

5.1. *Water Spray Cooling Failure Predictions*

Water supply failures are common in steel-plants. If the hydraulic system of a Stelmor machine is con-

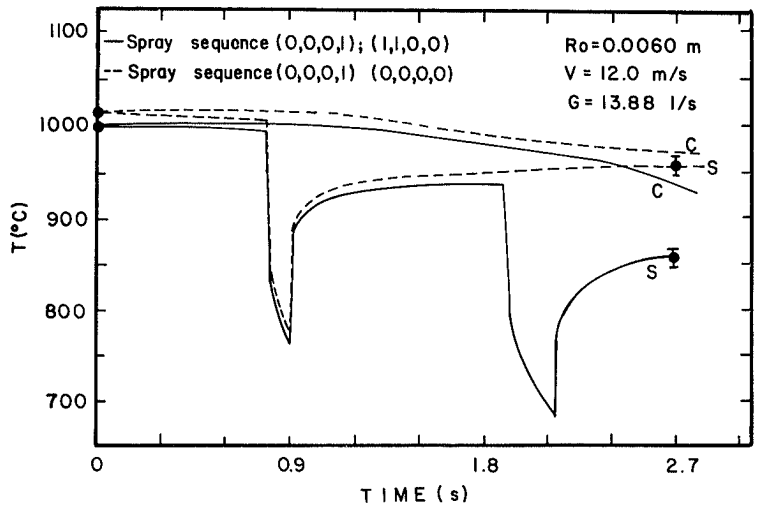

Fig. 7.
Simulation results of the RCS model as compared with experimental measurements under two quite different operation conditions.

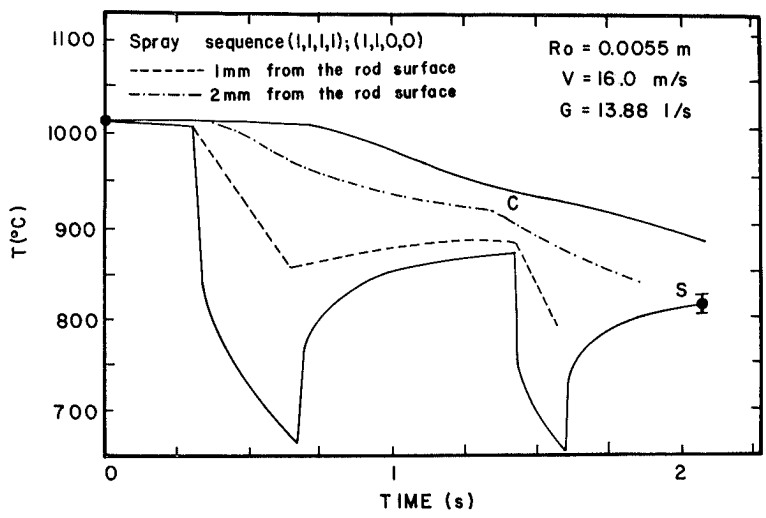

Fig. 8.
Rod cooling behavior at the RCS under extreme operating conditions.

nected to the steelmaking furnaces, continuous casting machine and mill roll cooling systems, then, it is possible to expect sudden changes in water supply pressures in the sprays of the RCS. According to the design of the RCS for this Stelmor machine, the flow-rate of water per-spray is 13.88 *l*/s as was previously mentioned. The calculation for a spray cooling sequence (1,1,0,0); (1,1,0,0) using that standard water flow-rate is presented in Fig. 9 for a 0.006 m rod radius. The rod center and rod surface temperatures at the end of the RCS (at the laying head) are 900 and 835°C, respectively. In Fig. 9 failures involving 75 and 50 % of that of the standard water flow-rate are presented.

In these calculations the rod center temperatures for the first and the second cases are 920 and 945°C, respectively, whereas the rod surface temperatures are 860 and 890°C, respectively. The reheating intensity seems to be decreased as the water flow-rate diminishes since the heat-transfer coefficient is directly related with the water flux as it can be seen from Eq. (I) in Table 3.

From this short analysis it can be concluded that a periodical inspection of water supply pressure and general conditions of the water delivering system in the RCS is badly needed if controlled and constant conditions want to be held.

Some other problems, different to those above mentioned, may arise during the operation of a Stelmor line. Sometimes the high carbon segregation at the rod center promotes the precipitation of cementite during patenting operations, and in order to avoid this, higher temperatures at the laying head are required. It is also a common case that, owing to a low cooling efficiency in the air forced cooling system, at the transformation conveyor, it is necessary to have the rod temperature as near as possible to the pearlite starting temperature. In the first case, moderate cooling conditions should be employed and in the latter, rather high cooling rates are to be applied. In either case a knowledge of the water supply system conditions is necessary, even if these conditions do not correspond to those considered as standard. This information should be fed to a model like this to be able to get the desired temperature at the laying head under any emergency situations.

5.2. *Effects of the Spray Cooling Sequence*

The spray cooling sequence influences directly the rod temperature profile at the laying head. To give a quantitative idea, calculations for three working sprays with different sequences were carried out. The operation conditions are clearly shown in Fig. 10. The (1,1,1,0); (0,0,0,0) cooling sequence gives a small difference between rod surface and center temperatures. The cooling pattern given by a sequence such as (0,0,1,1); (1,0,0,0) induces a higher difference between those two temperatures. However an extreme cooling sequence like (0,0,0,0); (0,1,1,1) can promote differences as big as 150–170°C between rod surface and center temperatures without any noticeable decrease of the rod center temperature.

Apparently, the magnitude of the temperature gradient across the rod radius seems not to be very important. Nevertheless, as it has been already shown,[24] a high temperature gradient may induce a partial pearlitic transformation outside the air forced cooling zone owing to a time consuming temperature equilibration phenomenon when the rod is already at the conveyor. This situation is particularly existent when rods with big radius (0.006 m) are being processed at the Stelmor machine.

Considering the deleterious effects that a partial transformation outside the air forced cooling zone may bring about on the mechanical properties of the final product, is highly recommendable to emphasize the convenience for choosing an adequate cooling sequence for the processing of big rod radius.

5.3. *Effects of the Initial Rod Temperature at the Last Roll of the Finishing Mill*

Fig. 11 shows the calculation results for a 0.006 m rod radius employing a (0,0,0,1); (1,1,0,0) spray cooling sequence. The compared initial temperatures are 1 030 and 1 060°C. The temperature gradient across the rod radius at the laying head position is the

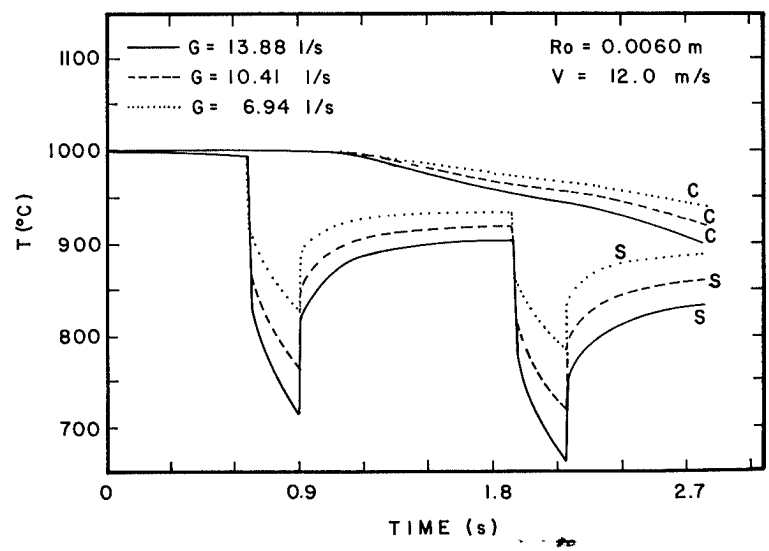

Fig. 9.
Water flow-rate effects on the rod cooling rates at the RCS.

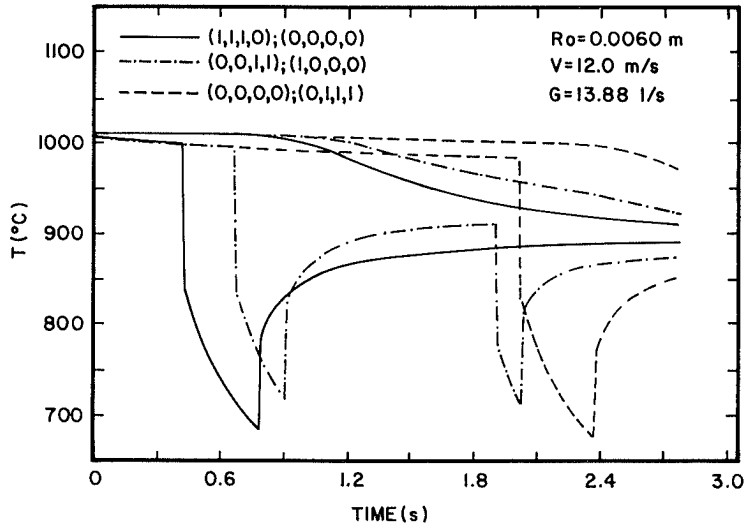

Fig. 10.
Temperature gradient across the rod radius as a function of the water spray cooling sequence.

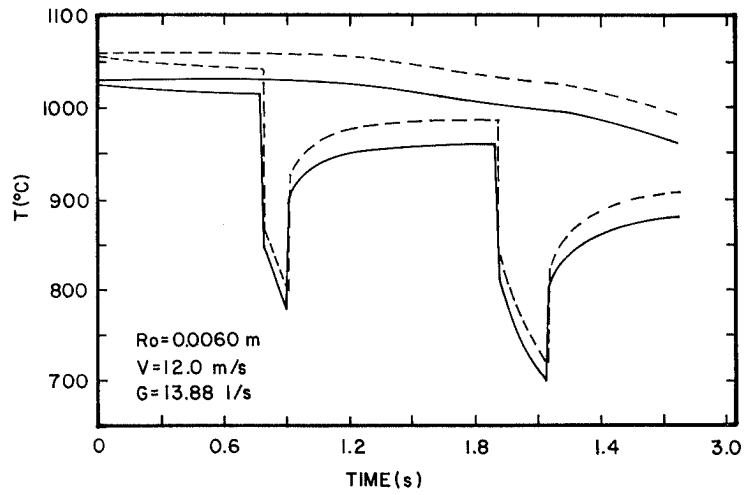

Fig. 11.
Effect of the rod temperature at the last roll of the finishing mill on the rod cooling behavior at the RCS.

same for both cases. Also, the rod surface temperature at the water spray working zones are almost the same for these two operating conditions. However, the reheating process promotes a more noticeable temperature difference at the rod surface if the rod is cooled from 1 030 or 1 060°C at the exit of the finishing block.

Obviously, the higher the initial temperature is the higher should be the number of working sprays to bring the rod temperature near to that of the pearlitic precipitation reaction.

5.4. Effects of the Rod Speed at the RCS

Modern steel rod finishing mills reach speeds as high as 100 m/s for a 0.0032 m rod radius. The higher speeds mean smaller residence times of a given volume element of the rod at the RCS line. Consequently, calculations for a 0.0032 m rod radius with different speeds at the RCS line were carried out. The corresponding results are presented in Fig. 12 for speeds lower (28 m/s) and higher (70 m/s) than that usually employed for this rod size (40–42 m/s, Table 1). Additional operation conditions are shown in Fig. 12.

The high rod speed under any given operation conditions will yield higher rod temperatures at the laying head position, as compared with the standard rod speed, lowering the RCS cooling efficiency. Additionally, for any rod size, higher speeds will produce higher temperature gradients between rod surface and rod center.

Low rod speeds will, naturally, work in the opposite direction.

6. Conclusions

A mathematical model which allows a thermal analysis of steel rods in a pre-cooling system (RCS) of a Stelmor machine has been developed. This model includes the influence of the principal operation parameters of the precooling system such as rod size, rod speed, initial rod temperature, water flow-rate and the spray cooling sequence. The prediction capacity of the model was validated with measured rod temperatures at HyLSA's Stelmor line. The key conclusions are summarized as follows:

(1) The model predictions and the measured data are in very good agreement.

(2) Reheating phenomena may go up to 200°C at rod surface, according with the model predictions, when steel rods are cooled down at the RCS. The magnitude of these reheatings are dependent on the

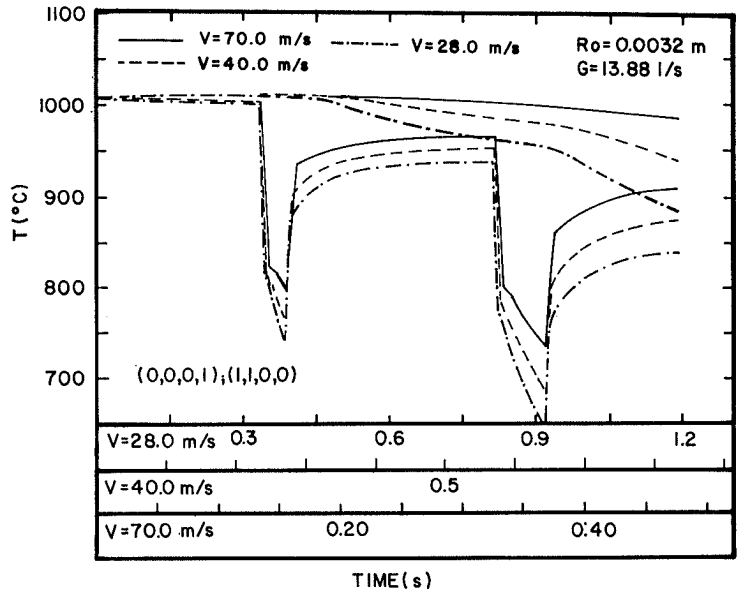

Fig. 12.
The rod cooling behavior at the RCS as a function of the rod speed.

cooling conditions and the rod radius.

(3) The cooling efficiency of the RCS is strongly dependent on the water flow-rate supplied to the cooling sprays. The heat transfer-coefficient at the spray cooling zone follows a simple linear relationship with water flux.

(4) The spray cooling sequence affects directly the temperature gradient across the rod diameter at the laying head position. Under cooling conditions where only the last 3 or 4 sprays are working while the rest of them are closed, the magnitude of this gradient increases without a noticeable rod center temperature decrease but with a strong rod surface temperature decrease.

(5) If a new and faster finishing block should be installed, the current RCS cooling efficiency should be critically reviewed.

Acknowledgments

The authors give the thanks to the Engineers E. Sánchez, L. Mosqueda, L. Contreras, J. Madrid, J. Sandoval and all operation personnel who facilitated the access to the plant and the experimental measurements. One of us (RDM) acknowledges also the financial support given by the Organization of American States and CoNaCyT to the Process Metallurgy Group at ESIQIE-IPN during the last five years and to Sistema Nacional de Investigadores for a granted scholarship.

REFERENCES

1) W. C. Leslie: The Physical Metallurgy of Steels, McGraw-Hill Book Co., New York, (1981), 169.
2) G. H. Geiger and D. R. Poirier: Transport Phenomena in Metallurgy, 1st Ed., Addison-Wesley Publ. Co., Reading, MA, (1973), 264.
3) Physical Constants of Some Commercial Steels at Elevated Temperatures, BISRA Scient. Publ., London, (1978).
4) J. R. Welty, R. E. Wilson and C. E. Wicks: Fundamentals of Momentum, Heat and Mass Transfer, John Wiley & Sons, New York, (1976), 733.
5) M. Mitsutsuka: *Tetsu-to-Hagané*, **69** (1983), 268.
6) H. Junk: *Neue Hütte*, **17** (1972), 13.
7) H. Müller and R. Jeschar: *Arch. Eisenhüttenwes.*, **44** (1973), 589.
8) M. Mitsutsuka: *Tetsu-to-Hagané*, **54** (1968), 1457.
9) E. A. Mizikar: *Iron Steel Eng.*, **47** (1970), 53.
10) M. Mitsutsuka and N. Fukuda: *Tetsu-to-Hagané*, **69** (1983), 262.
11) C. J. Hoogendoorn and R. den Hond: Proc. 5th International Heat Transfer Conference, paper B 3.12, Tokyo, Japan, (1974), 35.
12) K. Sasaki, Y. Sugitani and M. Kawasaki: *Tetsu-to-Hagané*, **65** (1975), 90.
13) H. Kamio, K. Kunioka and S. Sugiyama: *Tetsu-to-Hagané*, **63** (1977), S184.
14) T. Amano and A. Kamata: *Tetsu-to-Hagané*, **64** (1978), S254.
15) A. Ohtomo, M. Nakao and S. Yasunaga: *Tetsu-to-Hagané*, **67** (1981), S1041.
16) M. Ishiguro: *Tetsu-to-Hagané*, **60** (1974), S464.
17) T. Nozaki, J. Matsuno, K. Murata, H. Ooi and M. Kodama: *Trans. Iron Steel Inst. Jpn.*, **18** (1978), 330.
18) E. Bolle and J. C. Moreau: Proc. Int. Conf. on Heat and Mass Transfer in Metallurgical Processes, Dubrovnik Yugoslavia, (1979), 304.
19) M. Shimada and M. Mitsutsuka: *Tetsu-to-Hagané*, **52** (1966), 1643.
20) E. Bolle and J. C. Moreau: Proc. of Two Phase Flows and Heat Transfer, III, NATO Advanced Studies Inst., London, (1976), 1327.
21) Spe. Rep. No. 29 Kouzai-no Kyosei Reikyaku, ISIJ, Tokyo, (1977), 15.
22) W. M. Rosenhow: *Trans. ASME*, **74** (1952), 969.
23) B. V. Karlekar and R. M. Desmond: Transferencia de Calor, Ed. Interamericana, México D. F., (1985), 657.
24) A. G. López: MSc Thesis, Metallurgical Engineering Department of Metallurgy, ESIQIE-IPN, (1988).